Fe–TAML Encapsulated Inside Mesoporous Silica Nanoparticles as Peroxidase Mimic: Femtomolar Protein Detection

ARTICLE *in* ACS APPLIED MATERIALS & INTERFACES · AUGUST 2014

Impact Factor: 6.72 · DOI: 10.1021/am503275g · Source: PubMed

5 AUTHORS, INCLUDING:

Sushma Kumari
CSIR - National Chemical Laboratory, Pune
7 PUBLICATIONS **25** CITATIONS
SEE PROFILE

Chakadola Panda
Technische Universität Berlin
10 PUBLICATIONS **106** CITATIONS
SEE PROFILE

Abhishek Meena
Indian Institute of Technology Delhi
1 PUBLICATION **3** CITATIONS
SEE PROFILE

ACS APPLIED MATERIALS & INTERFACES

Research Article

www.acsami.org

Fe-TAML Encapsulated Inside Mesoporous Silica Nanoparticles as Peroxidase Mimic: Femtomolar Protein Detection

Sushma Kumari, Basab B. Dhar, Chakadola Panda, Abhishek Meena, and Sayam Sen Gupta*

CReST Chemical Engineering Division, National Chemical Laboratory, Pune-411008, India

Supporting Information

ABSTRACT: Peroxidase, such as horseradish peroxidase (HRP), conjugated to antibodies are routinely used for the detection of proteins via an ELISA type assay in which a critical step is the catalytic signal amplification by the enzyme to generate a detectable signal. Synthesis of functional mimics of peroxidase enzyme that display catalytic activity which far exceeds the native enzyme is extremely important for the precise and accurate determination of very low quantities of proteins (fM and lower) that is necessary for early clinical diagnosis. Despite great advancements, analyzing proteins of very low abundance colorimetrically, a method that is most sought after since it requires no equipment for the analysis, still faces great challenges. Most reported HRP mimics that show catalytic activity greater than native enzyme (~10-fold) are based on metal/metal-oxide nanoparticles such as Fe_3O_4. In this paper, we describe a second generation hybrid material developed by us in which approximately 25 000 alkyne tagged biuret modified Fe-tetraamido macrocyclic ligand (Fe-TAML), a very powerful small molecule synthetic HRP mimic, was covalently attached inside a 40 nm mesoporous silica nanoparticle (MSN). Biuret-modified Fe-TAMLs represent one of the best small molecule functional mimics of the enzyme HRP with reaction rates in water close to the native enzyme and operational stability (pH, ionic strength) far exceeding the natural enzyme. The catalytic activity of this hybrid material is around 1000-fold higher than that of natural HRP and 100-fold higher than that of most metal/metal oxide nanoparticle based HRP mimics reported to date. We also show that using antibody conjugates of this hybrid material it is possible to detect and, most importantly, quantify femtomolar quantities of proteins colorimetrically in an ELISA type assay. This represents at least 10-fold higher sensitivity than other colorimetric protein assays that have been reported using metal/metal oxide nanoparticles as HRP mimic. Using a human IgG expressing cell line, we were able to demonstrate that the protein of interest human IgG could be detected from a mixture of interfering proteins in our assay.

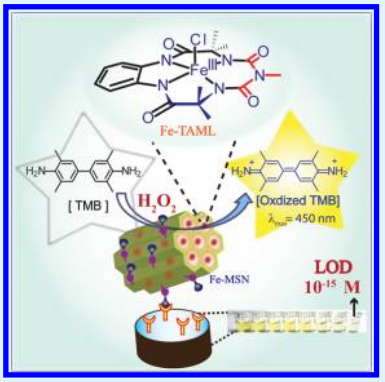

KEYWORDS: *MSN, peroxidase mimic, signal amplification, immuno assay, colorimetrically*

INTRODUCTION

Peroxidases such as the heme-containing horseradish peroxidase (HRP) is widely used for the detection of biomarker proteins where the key step is the peroxidase catalyzed conversion of a colorless substrate into a colored one, thus amplifying the signal many fold.[1,2] However, HRP conjugated to antibodies that are routinely used for protein detection via conventional enzyme-linked immunosorbent assay (ELISA type assay) has typical limit of detection (LOD) of ~10^{-12} M.[3,4] This LOD is significantly higher than what is necessary for ultrasensitive detection of proteins (~10^{-15} M or lower), which is essential for the early detection of several diseases.[5,6] It was envisioned that development of synthetic HRP mimics that possess higher K_{cat} values than native HRP could significantly bring down the detection limits, since the final signal-amplification would be enhanced several-fold. Out of several synthetic HRP mimics that have been successfully synthesized until date, nanomaterials with peroxidase activity have been quite successful. Ferromagnetic Fe_3O_4 nanoparticles (NPs) were the first that were discovered to possess peroxidase-like activity.[7] Subsequently, other nanomaterials having similar property such as cupric oxide NPs,[8] ceria NPs,[9] graphene oxide NPs,[10] and bimetallic NPs[11] such as Au@Pt[12] and Bi−Au[13] have also been reported. Antibodies have been attached on these nanoparticle surfaces and these conjugates have been used for the selective colorimetric detection of proteins with sensitivity limits, which are several fold lower than what can be achieved using their corresponding antibody-HRP conjugates.

Colorimetric detection of proteins in serum or cells is more preferred above other methods since it requires no equipment at all, which is useful for point-of-care (POC) applications[5] in settings that are resource-limited. Peroxidase mimic such as the 30 nm iron oxide NPs uses the $Fe^{2+/3+}$ ions[7] present on the surface to activate H_2O_2 to produce OH radical, which in turn oxidizes a peroxidase substrate such as 3,3′,5,5′-tetramethylbenzidine (TMB) to generate a visual signal. In contrast, a single active site in HRP generates a high-valent $Fe^{IV}O$ heme radical cation, which oxidizes TMB to its colored oxidized product. The higher peroxidase activity of 30 nm Fe_3O_4 NPs (~100-fold) is a result of large numbers of catalytically active

Received: May 26, 2014
Accepted: August 4, 2014
Published: August 4, 2014

Scheme 1. Schematic Representation of Signal Amplification

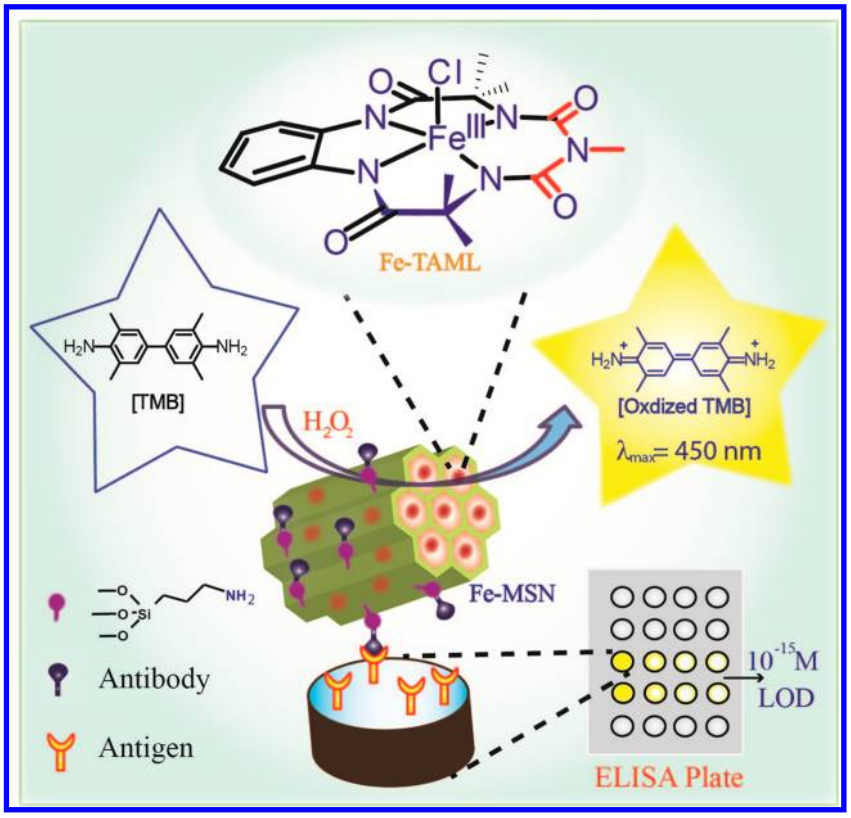

Fe ions (25 000 $Fe^{2+/3+}$ ions) present on its surface.[14] On a per-metal atom basis comparison between metal NPs and HRP, the $Fe^{2+/3+}$ ions in iron NPs oxide are much less efficient peroxidase mimic than the iron-porphyrin complexes in HRP. We had therefore hypothesized that if we are able to attach large numbers (e.g., ~25 000) of small molecule functional mimic of HRP inside a porous NP, their activity would likely far exceed that of the metal/metal oxide NPs too. Further, outer surface of NPs (especially silica) allows easy chemical modifications to install targeting groups such as antibodies. Such a conjugate can then be used for biomolecule detection in ELISA type assays with detection limits that should be far lower than the corresponding antibody-metal NP conjugates. This would also represent a truly biomimetic system since the HRP mimic embedded inside a NP would resemble an enzymatic system.

The choice of an efficient small molecule peroxidase mimic therefore becomes critical in designing such systems discussed above. Fe complex of tetra-amidomacrocyclic ligands (Fe-TAML) developed by Collins,[15−17] represents by far the most efficient small molecule (Mol wt ~ 500 g/mol) peroxidase mimic having reactivity nearly the native enzymes. We have recently synthesized and reported a biuret modified Fe-TAML complex which displayed excellent reactivity and very high stability, especially at low pH and high ionic strength in comparison to the prototype Fe-TAML.[18,19] This biuret modified Fe-TAML forms the corresponding room temperature stable $Fe^{V}(O)$ in the presence of oxidant and has been shown to oxidize a variety of alkanes via C−H abstraction.[20] A variation of this biuret modified Fe-TAML that was attached inside Mesoporous Silica Nanoparticles (MSN; diameter 100 nm) showed good peroxidase activity and was used for selective detection of glucose and cyanide.[21,22] In this paper, we report a much improved Fe-TAML embedded[21,22] MSN construct that has peroxidase activity that is around 1000-fold higher than that of the particles that has been reported by us before. It is activity is also around 100-fold more than that of metal/metal-oxide NPs that have been reported before.[5] We also show that the outer surface of these peroxidase mimics can be conjugated to an antibody such as antihuman IgG on the exterior of Fe-MSN thus maximizing the ratio of antibody to biuret modified Fe-TAML. This high ratio allows these particles to detect human immunoglobulin (human IgG) up to concentration of 1 pg/mL (~10^{-15} M) via an ELISA type colorimetric assay. This represents a 1000-fold increase in sensitivity over using commercial antihuman IgG-HRP[3,4] conjugate. We also report the selective detection of human IgG from cells that were genetically engineered to express IgG using the whole cell lysate demonstrating that high background proteins do not interfere with our assay.

EXPERIMENTAL SECTION

Kinetics of TMB Oxidation. The determination of K_m and K_{cat} values of 1-Fe-MSN and 5-Fe-MSN for the oxidation of TMB in the presence of H_2O_2 was carried out at the physiological pH 7.4. For kinetic runs, primary stock solutions of 5-Fe-MSN (0.5 μg/mL) and 1-Fe-MSN (2 μg/mL) was prepared in deionized water. In all kinetic runs the amount of 1-Fe-MSN or 5-Fe-MSN added was kept constant. Concentration of H_2O_2 was calculated by measuring the UV−vis absorbance at 240 nm (ε = 43.6 M^{-1} cm^{-1}). To investigate the peroxidase activity of 1-Fe-MSN, TMB concentration was fixed at 1.6 × 10^{-4} M while H_2O_2 was varied from 4.8 × 10^{-3} to 32 × 10^{-3} M. For TMB variation, the reverse procedure was followed ([H_2O_2] = 10.0 × 10^{-3} M; [TMB] = 2.4 × 10^{-5} − 3.2 × 10^{-4} M). Similarly, for 5-Fe-MSN H_2O_2 was varied from 3 × 10^{-3} to 40 × 10^{-3} M while keeping the TMB concentration fixed at 2 × 10^{-4} M. TMB was varied from 5.0 × 10^{-5} − 4.0 × 10^{-4} M while keeping the [H_2O_2] constant at 8.0 × 10^{-3} M. PBS buffer (pH 7.4; 10 mM) was used for all the kinetic runs.

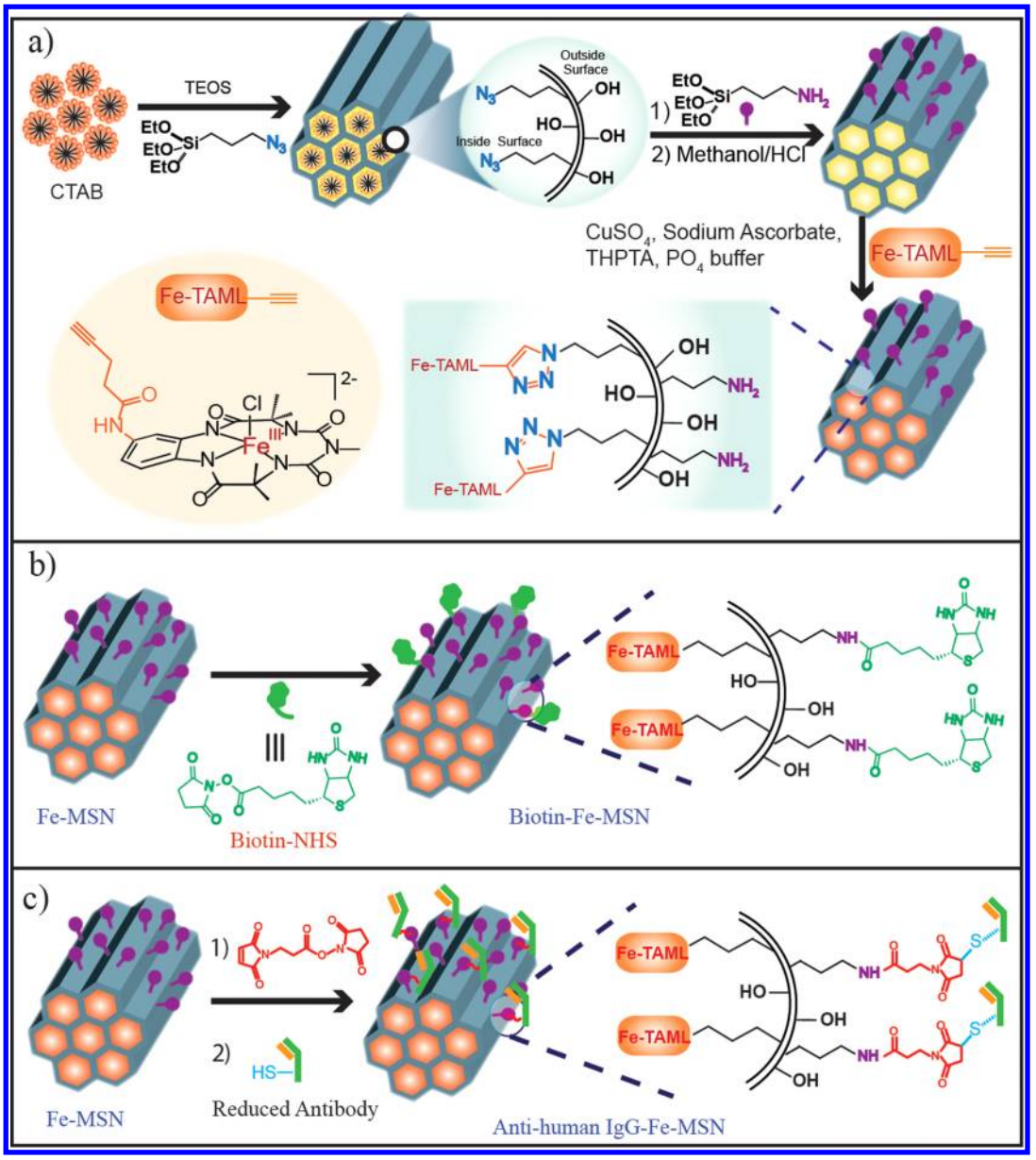

Figure 1. Synthesis of (a) biuret modified Fe-TAML functionalized MSN (Fe-MSN); (b) biotin conjugated Fe-MSN; (c) antihuman IgG conjugated Fe-MSN.

Colorimetric Assay of Streptavidin. In ELISA for the detection of streptavidin, 96-well polystyrene (PS) plates were used. For a typical ELISA experiment, 100 μL of streptavidin with concentrations ranging from 0.001 to10^5 ng/mL was added to each well and incubated at 4 °C overnight. After incubation, the plate was washed three times with 100 mM pH 7.4 PBS buffer. Each well was filled with 100 μL of 1% BSA in PBS as blocking agent to prevent nonspecific interaction between the plate and biotin conjugated Fe-MSN. After 2 h, the plate was decanted and washed three times with PBS buffer. In the second step, 50 μL of biotin-Fe-MSN (10^{-2} mg/mL) was added into wells and incubated at 37 °C for another 1 h. After washing three times with PBS buffer, 100 μL substrate stock solution containing TMB (4×10^{-5} M) and H_2O_2 (16×10^{-3} M) was added to each well. After 10 min of incubation, the green color observed was immediately quenched with 0.1 N HCl. ELISA reading was performed in a microplate reader at 450 nm.

Detection of Human IgG Using Antihuman IgG-Fe-MSN. The detection of human IgG using antihuman IgG-Fe-MSN was performed by the standard sandwich ELISA format included coating a 96-microwell plate with affinity purified rabbit antihuman IgG for capture of IgG. Then, each well was filled with 100 μL of 1% BSA in PBS and incubated at 37 °C for another 2 h to prevent nonspecific interactions between the plate surface and antibody conjugated Fe-MSN, followed by incubating the protein human IgG (100 μL of 10^{-3} to10^5 ng/mL) at 37 °C for 3 h. After incubation, the plate was washed three times with PBS and then 50 μL of antihuman IgG-Fe-MSN (10^{-2} mg/mL) was added into the wells and incubated for an additional hour. The color development was initiated by addition of 100 μL of TMB (4×10^{-5} M) and H_2O_2 (16×10^{-3} M). After 10 min of incubation, the green color observed was immediately quenched with 0.1 N HCl. ELISA reading was performed in a microplate reader at 450 nm.

Detection of Human IgG in CHO-S and CHO-IgG. CHO-S and CHO-IgG cells were grown in suspension under 10% CO_2 atmosphere at 37 °C. Cells suspension was centrifuged and washed with an ice-cold PBS to remove the excess media. The cell pellet was lysed by suspension in ice-cold lysis buffer for 15 min, centrifuged and the supernatant was collected for further assay. Supernatant containing CHO-S and CHO-IgG cells were diluted to 10^5, 10^4, and 10^3 cells/mL and were plated on 96 well plates by incubation at 4 °C for 24 h. The plates were further incubated with antihuman IgG-Fe-MSN for

another 1 h, subsequently washed several times and then probed with TMB (4×10^{-5} M) and H_2O_2 (16×10^{-3} M). After 10 min, the reaction was quenched with 0.1 N HCl. ELISA reading was performed in a microplate reader at 450 nm.

RESULTS AND DISCUSSION

Design and Synthesis of Biuret Modified Fe-TAML Immobilized MSN. Detection of biomolecules in femtomolar concentration necessitates development of particles that possess very high peroxidase activity and is also capable of multivalently displaying receptor ligands (e.g., antibodies for protein detection) on its surface. We therefore designed a MSN that contained several chemically conjugated HRP mimic biuret modified Fe-TAML inside the pores and antibody molecules on its surface (Scheme1). The presence of large number of biuret modified Fe-TAML complexes inside MSN is expected to have an additive effect to their individual activity and therefore increase the overall peroxidase activity in comparison to HRP enzyme. This high peroxidase activity together with the increased binding affinity of Fe-MSN to the target protein due to multivalent display of antibodies on its surface is expected to bring down the detection limits several-fold in comparison to commercial antibody-HRP conjugates.

We have previously reported the synthesis of Fe-(biuret) TAML modified MSN (Fe-MSN) in which 100 nm MSN containing 1% azidopropyl group was used to attach biuret modified Fe-TAML using CuAAC (1st generation Fe-MSN).[21] However, their tendency to aggregate in aqueous solution and the low peroxidase activity (due to low loading of biuret modified Fe-TAML) in comparison to commercial HRP made them unsuitable for usage as catalysts for signal amplification at low nanoparticle concentration conditions that are necessary for ultrasensitive detection of proteins via ELISA type assays. We therefore proceeded to design a second generation Fe-MSN construct that would possess much improved peroxidase activity and will also be amenable to external modification with receptor molecules such as antibodies. We hypothesized that a smaller mesoporous nanoparticle (smaller than first generation Fe-MSN which had 100 nm diameter) and increased amounts of biuret modified Fe-TAML loading (greater 0.05 mmol/g as in first generation Fe-MSN) would probably maximize peroxidase activity and will increase its ability to disperse well in aqueous solutions. Further presence of aminopropyl groups exclusively on the outer surface would allow easy attachment of receptor molecules such as antibodies on Fe-MSN. Our synthetic strategy is therefore based on a bioorthogonal approach consisting of the following steps: (1) Synthesis of azido-functionalized MSN particles (N_3-MSN) with average diameter of 30−40 nm using a co-condensation approach so that most of the azidopropyl groups are present inside the MSN; (2) Grafting of amino propyl group on the as-synthesized MSN followed by template removal and (3) Attachment of biuret modified Fe-TAML to N_3-MSN using CuAAC (Figure 1a).

We attempted the synthesis of azide grafted spherical MSN[21,23,24] having average diameter between 30 and 40 nm by the co-condensation method. This is likely to result in the organo azide group residing mostly inside the pores. The reasons for this can be attributed to the following: (i) Considering that the azidopropyl group is randomly distributed over the whole material, the higher internal to external surface area ratio (7:1) would lead to the azidopropyl group being located mostly inside the pore. (ii) During initial formation of the first layer of silica during our synthesis, the azidopropyl group (from AzPTES) will be located inside the surfactant as has been discussed before for the synthesis of a related material.[21b] Condensation of TEOS to form silica walls will then subsequently occur over this first layer. We believe this model to be true for the synthesis of our material as >95% azides are available for subsequent conversion into the corresponding triazoles using CuAAC with small molecule alkynes as the substrate. This indirectly shows that the hydrophobic azidopropyl group was embedded inside the surfactant during initial silica condensation thus ending up mostly inside the pores. The amount of azide grafted was varied from 1 to 10% to allow us to study the effect of biuret modified Fe-TAML loading on peroxidase activity. The resultant azide grafted MSN containing 1, 5, and 10% azidopropyl groups (1-N_3-MSN, 5-N_3-MSN, and 10-N_3-MSN, respectively) obtained after template removal was thoroughly characterized by several physical techniques. The material was found to be very stable in water (pH 4−9) and high ionic strength (phosphate buffer 100 mM). Transmission electron microscopy (TEM), X-ray diffraction (XRD), and scanning electron microscopy (SEM) of N_3-MSN showed formation of well-ordered two-dimensional hexagonal MSN with a spherical morphology having average particle size of ∼40 nm (Supporting Information (SI) Figures 1, 2, and 3). Nitrogen adsorption−desorption showed high surface area and the average pore size was determined to be near 3 nm (Table 1, SI Figures 5, 6, and 7). The presence of the azido functional group was confirmed by Fourier transform infrared (FT-IR) (absorbance at ∼2100 cm^{-1}) and by ^{13}C CP MAS NMR spectrum (three peaks at 8.68 ppm, C2 22 and 53 ppm) as has been described before (SI Figures 8, 9, 10, and 12). TGA analysis showed the amount of azidopropyl groups incorporated onto 1-N_3-MSN, 5-N_3-MSN, and 10-N_3-MSN to be 0.14, 0.51, and 0.90 mmol/g respectively (Table 1, SI Figure 13). Biuret modified Fe-TAML containing an alkyne group was then attached to N_3-MSN using a modified CuAAC procedure. The qualitative and quantitative incorporation of biuret modified Fe-TAML was studied using FT-IR, electron paramagnetic resonance (EPR), and inductively coupled plasma (ICP) analysis (SI Figures 8, 9, 10, and 11). From ICP analysis, the biuret modified Fe-TAML incorporation was estimated to be 0.15, 0.64, and 0.77 mmol/g of Fe-MSN. The IR results show that the extent of CuAAC for the grafting of biuret modified Fe-TAML onto 1-N_3-MSN and 5-N_3-MSN was greater than 95%. In contrast, for 10-N_3-MSN the extent of CuAAC was found to be only 85%. In fact, the amount of biuret modified Fe-TAML did not increase much when the azide incorporation was increased from 5 to 10% (most likely for steric reasons). In lieu of this, only biuret modified Fe-TAML attached to 1-N_3-MSN and 5-N_3-MSN (1-Fe-MSN and 5-Fe-MSN, respectively) was further evaluated for their peroxidase activity (Table 2; for K_{cat} values of 10-Fe-MSN see SI Figure 17). Finally, the density of 1-N_3-MSN and 5-N_3-MSN was estimated from the N_2 adsorption−desorption data to evaluate

Table 1. Physical Properties of x-N_3-MSN

x-N_3-MSN	N_3 grafting density (mmol/g)	surface area M_{BET} (m^2/g)	pore diam. (nm)	pore vol. (cc/g)
1-N_3-MSN	0.14	947	3.54	0.925
5-N_3-MSN	0.51	851	3.30	0.779
10-N_3MSN	0.90	824	3.18	0.731

Table 2. Comparison of the Kinetic Parameters of 1-Fe-MSN, 5-Fe-MSN, HRP, 30 nm Fe_3O_4 MNPs, and Au@Pt 0.25[a]

	[E] (M)[b]	substrate	K_m (mM)	V_{max} (Ms^{-1})	K_{cat} (s^{-1})	K_{cat}/K_m (s^{-1} M^{-1})
1-Fe-MSN	7.92×10^{-13}	TMB	0.033	1.297×10^{-7}	1.64×10^{5}	4.97×10^{9}
1-Fe-MSN	7.92×10^{-13}	H_2O_2	9.617	1.785×10^{-7}	2.25×10^{5}	2.3×10^{7}
5-Fe-MSN	1.25×10^{-13}	TMB	0.122	3.316×10^{-7}	2.65×10^{6}	2.17×10^{10}
5-Fe-MSN	1.25×10^{-13}	H_2O_2	6.67	3.267×10^{-7}	2.60×10^{6}	3.89×10^{8}
1st-Fe-MSN[21]	2.6×10^{-11}	TMB	0.016	1.01×10^{-8}	4.00×10^{2}	2.47×10^{7}
HRP[7]	2.5×10^{-13}	TMB	0.434	10.00×10^{-8}	4.00×10^{3}	9.22×10^{6}
30 nm Fe_3O_4 MNPs[7]	11.4×10^{-13}	TMB	0.098	3.44×10^{-8}	3.02×10^{4}	3.08×10^{8}
Au@Pt 0.25[12]	12.5×10^{-12}	TMB	0.027	1.81×10^{-7}	1.4×10^{4}	5.18×10^{8}

[a][E] is the enzyme (Au@Pt 0.25 or Fe-MSN or MNPs) concentration, K_m is the Michaelis–Menten constant, V_{max} is the maximal reaction velocity, and K_{cat} is the catalytic constant, where $K_{cat} = V_{max}/[E]$. [b]Concentrations have been calculated for 1-Fe-MSN and 5-Fe-MSN from TEM, ICP, and N_2 adsorption–desorption data (see SI Figure 2).

the number of biuret modified Fe-TAMLs incorporated in each nanoparticle. It was estimated that around 25 000 and 5000 biuret modified Fe-TAMLs were covalently attached inside 5-Fe-MSN and 1-Fe-MSN, respectively.

Evaluation of Kinetic Parameters for TMB Oxidation by Fe-TAML Encapsulated in MSN. The peroxidase activity of 1-Fe-MSN, 5-Fe-MSN, and 10-Fe-MSN were evaluated by studying their efficiency for the H_2O_2 mediated oxidation of TMB to form colored oxidized products. The oxidation reaction was carried out at the physiological pH of 7.4 and the kinetic parameters V_{max}, K_{cat}, and K_m were determined (Table 2). These three parameters were chosen so that the activity of the whole particle Fe-MSN can be compared with both HRP and other metal/metal oxide based NPs that have been reported.[7] At pH 7.4 upon oxidation, TMB forms three products (TMB^{2+}, oxidized TMB charge transfer complex and TMB^{+}), which remain in equilibrium.[25] However, when the pH of the solution is lowered below 2, the equilibrium is shifted toward the complete formation of TMB^{2+} (characteristic peak at 450 nm; ε = 59 000 $M^{-1}cm^{-1}$) together with the disappearance of oxidized TMB charge transfer complex and TMB^{+} (SI Figure 16). Therefore, for all kinetic runs the reactions were initiated at pH 7.4 but were quenched to pH < 2 by addition of HCl at different time intervals and the absorbance was measured at 450 nm. The plots of initial rate vs substrate concentrations were fitted perfectly to a typical Michaelis–Menten curve (SI Figure 17) and the K_m and V_{max} values were determined (Table 2). The K_{cat} values of 5-Fe-MSN with TMB as the substrate was found to be 10-folds higher than 1-Fe-MSN. Similarly, the catalytic efficiency (K_{cat}/K_m) of 5-Fe-MSN with TMB as the substrate was found to be 4-folds higher than 1-Fe-MSN. This demonstrated that increasing the loadings of biuret modified Fe-TAML inside MSN led to increased catalytic efficiency. In comparison to our first generation Fe-MSN,[21] 5-Fe-MSN displayed a K_{cat} value 1000-fold higher. Hence, reduction of nanoparticle size (thereby increasing surface area and dispersibility) and increase in biuret modified Fe-TAML content had a huge positive effect on the catalytic activity for our second generation Fe-MSN. The effect of pH on the catalytic efficiency of the reaction was also studied. It was determined that the amount of oxidized TMB formed at the end of the reaction (responsible for peaks at 450, 650, and 900 nm) was lower at pH 6 and pH 8.4 than at pH 7.4 (SI Figure 15). This can be rationalized by careful understanding of the mechanism of Fe-TAML mediated oxidation reactions in water. It is well established that the rate of substrate oxidation by Fe-TAML and H_2O_2 increases with increasing pH and hence the activity of 5-Fe-MSN gets reduced at pH 6.[26] At pH 7.4 in the presence of peroxide, Fe-TAML forms a μ-O-Fe^{IV} dimer species that is responsible for the 2-electron oxidation of TMB.[27] However, with increasing pH, the μ-O-Fe^{IV} dimer species gets converted to $Fe^{IV}(O)$, which is far more active oxidant.[27] Hence at pH 8.4, although oxidized TMB species is formed at faster rates, they undergo subsequent oxidation reactions to form degradation products which are colorless. Fe-TAML is very well-known to completely degrade recalcitrant organic compounds[28] at higher pH. Hence, pH 7.4 was considered as the most optimal for obtaining the highest catalytic efficiency.

On comparison of 5-Fe-MSN and 1-Fe-MSN to HRP, it can be seen that K_{cat}/K_m values were 2300 times and 540 times higher than those of commercial HRP, respectively. Among the metal nanoparticles, the highest K_{cat} values have been observed for 30 nm Fe_3O_4 and Au@Pt 0.25 NPs.[12] The K_{cat} value of 5-Fe-MSN is around 100-fold higher than that of both 30 nm iron oxide and Au@Pt 0.25 NPs. This is expected because biuret modified Fe-TAML has peroxidase activity that is far superior to that of the metal ions present on the nanoparticle surface. This 2300-fold increased peroxidase activity of 5-Fe-MSN in comparison to HRP encouraged us to use this nanoparticle for ultrasensitive detection of proteins.

Biotin Conjugated Fe-MSN for Detection of Streptavidin. The detection of streptavidin was attempted using biotin modified 5-Fe-MSN. Streptavidin is known to bind biotin with very high specificity (10^{-14} mol/L).[29] We hypothesized that using 5-Fe-MSN that would have biotin displayed on its surface would help us to detect streptavidin in an conventional ELISA assay in which commercially used biotin-HRP would be replaced with our biotin conjugated 5-Fe-MSN. We therefore proceeded to synthesize 5-Fe-MSN having biotin displayed on its surface. This was achieved by first grafting 3-aminopropyl triethoxysilane onto the as synthesized 5-N_3-MSN followed by template removal (Figure 1a). Biuret modified Fe-TAML was then "clicked" onto NH_2–N_3-MSN using CuAAC and the resultant material NH_2–Fe-MSN was characterized by FT-IR, thermogravimetric analysis (TGA), and ICP (Figure 1, SI Figures 9 and 14). The amount of amine groups grafted was estimated to be 1.04 mmol/g while the amount of biuret modified Fe-TAML grafted was determined to be 0.51 mmol/g. TEM image shows the absence of clustering in mesoporous silica nanoparticles after surface modification. Additionally, ninhydrin test was done to confirm amine groups on the surface of 5-N_3-MSN (SI Figure 3). Finally, NH_2-Fe-MSN was reacted with biotin-NHS to yield biotin-Fe-MSN which was then used for the detection of streptavidin (Figure 1b).

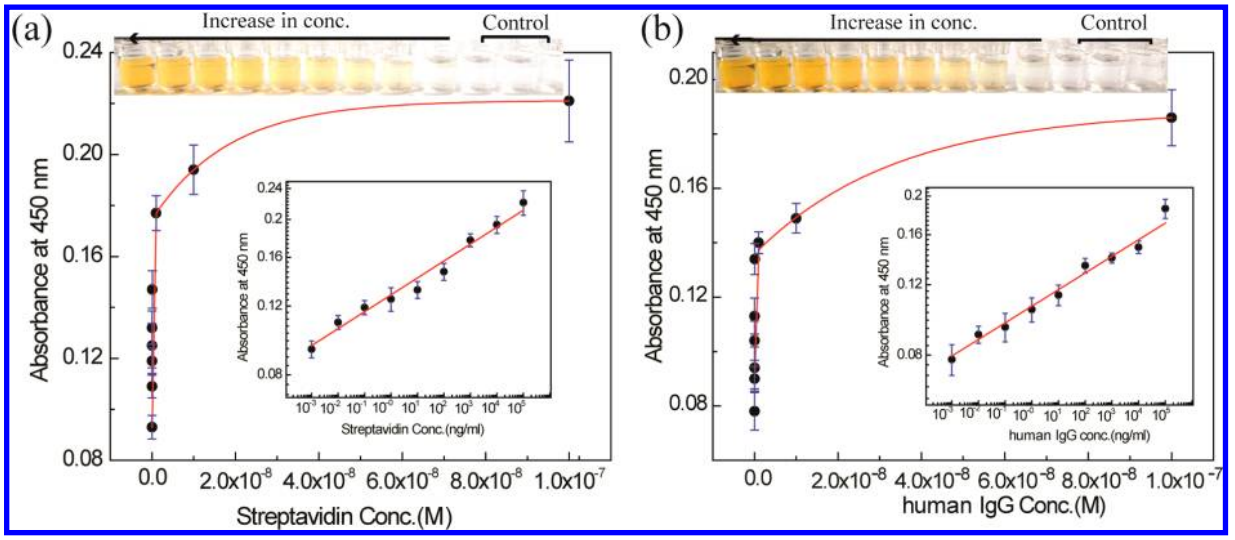

Figure 2. Application of biuret modified Fe-TAML MSN in direct immunosorbent assay. (a) Calibration curve for the detection of streptavidin in various concentration from 1 pg/mL to 10^6 ng/mL using biotin conjugated Fe-MSN in a 96-well plate. (b) Calibration curve of the immunosorbent assay for the detection of human IgG in various concentration from 1 pg/mL to 10^6 ng/mL using antihuman IgG conjugated Fe-MSN. The error bars represent the standard deviation from triplicate measurements.

A 96-well plate was first coated with streptavidin (0.001 to 10^5 ng/mL), then blocked with 1% BSA, and finally incubated with biotin conjugated 5-Fe-MSN for 1 h. After several washes to remove nonspecific binding, the substrate TMB and H_2O_2 were added such that the biotin conjugated 5-Fe-MSN bound to the streptavidin can utilize H_2O_2 to catalyze the formation of colored oxidized TMB. The reaction was measured using an ELISA plate reader at 450 nm. A linear dependence of absorbance vs analyte concentration was obtained in the range of 1 pg/mL to 10^6 ng/mL (log [absorbance] vs log [streptavidin]) with a limit of detection (LOD) of 19 fM (Figure 2a). Control experiments in which N_3-MSN or Fe-MSN was used as the probe in place of biotin-Fe-MSN, showed no detectable signal. In the lowest detection limit, the signal was at least twice that was obtained when BSA was used instead of streptavidin as a control. These initial results encouraged us to explore the detection of human IgG in an ELISA format using antihuman IgG conjugated Fe-MSN as the probe.

Antihuman IgG Conjugated Fe-MSN for Detection of Human IgG in Cells. To evaluate the efficiency of this highly active peroxidase mimic, the ultrasensitive detection (fM) and quantification of human IgG protein was attempted. The amine groups on the surface of NH_2-Fe-MSN were converted to maleimides onto which antihuman IgG was attached using the thiol-maleimide chemistry as shown in (Figure 1c, SI Scheme 1). Any unreacted maleimide on the surface of Fe-MSN was quenched by addition of cysteine. For colorimetric immunoassay of human IgG, several concentrations of human IgG (0.001 to 10^5 ng/mL) were captured on 96-well plate and then subsequently incubated with antihuman IgG-Fe-MSN for 1 h. After several washes to remove nonspecific binding of antihuman IgG-Fe-MSN, TMB and H_2O_2 were added. After 10 min, the reaction was quenched with addition of HCl and the absorbance at 450 nm was measured. Figure 2b shows the correlation between the signals generated at 450 nm vs human IgG concentration. The results show a linear relationship in the range from 10^{-12} to 10^{-4} g/mL and the limit of detection is 10^{-12} g/mL (6×10^{-15} M). Control experiments in which N_3-MSN or Fe-MSN was used as the probe in place of antihuman IgG-Fe-MSN showed no detectable signal. In the lowest detection limit, the signal was at least twice that was obtained when BSA was used instead of human IgG as a control. In contrast, when the same assay was carried out with commercially used antihuman IgG-HRP conjugate, linearity was only observed in the range from 10^{-8} to 10^{-4} g/mL (log [absorbance] vs log [human IgG]) and the LOD was 10^{-8} g/mL (6.7×10^{-11} M).[30] In other words, the use of antihuman IgG-Fe-MSN allows us to probe a dynamic range of human IgG that is at least 4 orders of magnitude higher than that which can be probed with commercial antihuman IgG-HRP. Hence, the ultrasensitive detection of human IgG at femtomolar concentrations can be achieved using our designed antihuman IgG-Fe-MSN. In comparison, the LOD for metal NP based peroxidase mimic (e.g., Au@Pt 0.25) for the detection of mouse interleukin 2 (IL-2) has been reported to be $\sim 10^{-11}$ g/mL, which was 10-fold higher than that has been achieved by our system. In another approach, MSN with antibody immobilized on the outer surface and the enzyme glucose oxidase (GO) immobilized inside was used for detection of proteins.[31] The LOD for this system was observed to be 100 pg/mL. This is also 100 times higher than our reported construct. The low detection limit for our antihuman IgG-Fe-MSN is results of 25 000 extremely efficient peroxidase mimic biuret modified Fe-TAML, which was immobilized inside MSN.

A major challenge in ultrasensitive detection of proteins in cells is the identification of specific proteins among a high background of interfering proteins that are present in real samples. To further evaluate if antihuman IgG-Fe-MSN could specifically detect human IgG from a high background of interfering proteins, we attempted the assay using two different cell lines of Chinese hamster ovary cells (CHO-S and CHO-IgG). CHO-IgG cell lines express human IgG while CHO-S cells do not express human IgG.[30] Both CHO-S and CHO-IgG cells were grown in suspension under 10% CO_2 atmosphere at 37 °C. Cells suspension was centrifuged and washed with an ice-cold PBS to remove the excess media. The cell pellet was lysed by suspension in ice-cold lysis buffer for 15 min and centrifuged, and the supernatant was collected for further assay. Supernatant containing CHO-S and CHO-IgG cells were diluted to 10^5, 10^4, and 10^3 cells/mL and were plated on 96

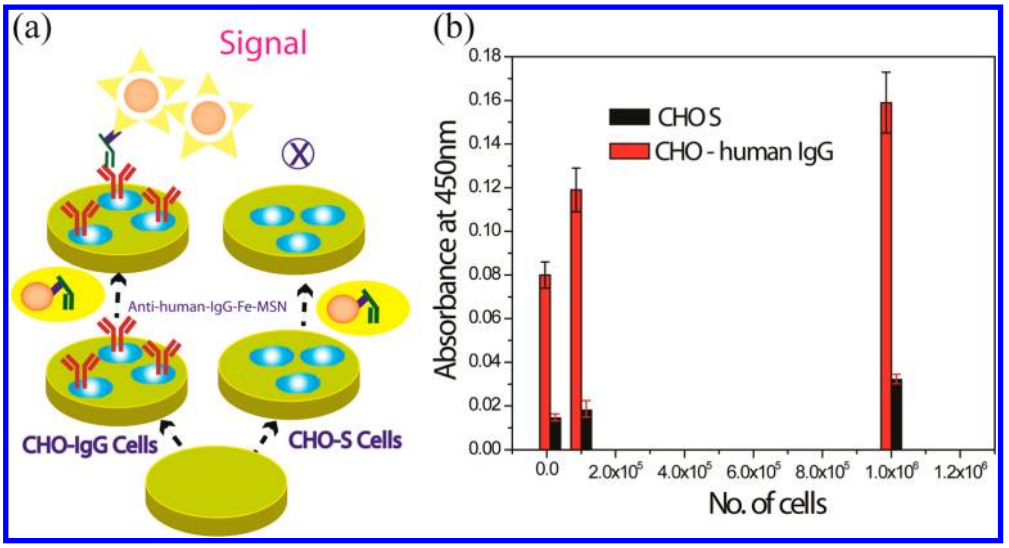

Figure 3. Human IgG detection in CHO-S and CHO-IgG cells. (a) Schematic representation of the proposed strategy for cell detection in a 96-well plate. (b) Specificity and sensitivity of antihuman IgG-Fe-MSN for CHO-S and CHO-IgG cells were evaluated by assaying 10^5, 10^4, and 10^3 cells/mL in a 96 well plate format. The error bars represent the standard deviation from triplicate measurements.

well plates by incubation at 4 °C for 24 h. The plates were further incubated with antihuman IgG-Fe-MSN for another 1 h and then washed several times to remove unbound antihuman IgG-Fe-MSN. Finally, TMB and H_2O_2 were added, the reaction was subsequently quenched with HCl, and the absorbance of the resultant solution was measured at 450 nm. The presence of a signal was only absorbed for CHO-IgG cells while for CHO-S cells no signal was observed (Figure 3). The signal-to-noise ratio for 10^3 cells is at-least 4-fold. This conclusively demonstrates that antihuman IgG-Fe-MSN was able to detect human IgG selectively from high background of other proteins present in CHO cells.

CONCLUSIONS

In a biomimetic approach we have chemically attached ~25 000 highly active small molecule peroxidase mimic biuret modified Fe-TAML inside a 40 nm mesoporous nanoparticle. One of our constructs, 5-Fe-MSN, possess a K_{cat}/K_m value that is ~2300-fold higher in comparison to commercial HRP and 100-fold higher than metal/metal oxide NPs that have been reported. The presence of silanol groups in the outer surface of 5-Fe-MSN allowed easy attachment of biotin and the antibody antihuman IgG. This surface modified 5-Fe-MSN was used for the ultrasensitive detection of proteins. Using antihuman IgG modified 5-Fe-MSN, we were able to detect femtomolar concentration of antihuman IgG. We were also able to quantify human IgG within a dynamic range of nanomolar to femtomolar concentrations. This represents a sensitivity that is 1000-fold higher than that of commercial antihuman IgG-HRP and 10-fold higher than that of any metal/metal oxide peroxidase mimic that has been reported to date. The understanding of the mechanism of the catalytic acitivity of biuret modified Fe-TAML will allow us to develop a new generation Fe-MSN, which will have increased catalytic efficiency. For example, Fe-TAML, which has a maximal activity at pH 7.4, can be used using design rules that have been developed by Collins.[17] Such systems are currently under development in our laboratory.

ASSOCIATED CONTENT

Supporting Information

Synthesis and detailed characterization of functionalized Fe-MSN, kinetics of TMB oxidation and spectra, experimental details of colorimetric assay. This material is available free of charge via the Internet at http://pubs.acs.org.

AUTHOR INFORMATION

Corresponding Author

*Email: ss.sengupta@ncl.res.in. Fax: +91 20 25902621. Tel: +91 20 25902747.

Author Contributions

The manuscript was written through contributions of all authors. All authors have given approval to the final version of the manuscript.

Funding

S.S.G. thanks network project CSIR 12th FYP Network Project CSC0134 for funding. S.K. and C.P. thank CSIR, New Delhi for fellowship. B.B.D. acknowledges CSIR for SRA (Scientist, Pool Scheme, CSIR) position.

Notes

The authors declare no competing financial interest.

ACKNOWLEDGMENTS

We thank Prof. Michael Kruk (CUNY) with help regarding determination of density of MSN's. We are also thankful to Dr. Mugdha Gadgil for help regarding CHO-S and CHO-IgG cells.

REFERENCES

(1) Marquez, L. A.; Dunford, H. B. Mechanism of the Oxidation of 3,5,3′,5′ Tetramethyl-benzidine by Myeloperoxidase Determined by Transient- and Steady-State Kinetics. *Biochemistry* **1997**, *36*, 9349−9355.

(2) Whitehead, T. P.; Thorpe, G. H. G.; Carter, T. J. N.; Groucutt, C.; Kricka, L. J. Enhanced Luminescence Procedure for Sensitive Determination of Peroxidase-Labelled Conjugates in Immunoassay. *Nature* **1983**, *305*, 158−159.

(3) Engvall, E.; Perlmann, P. Enzyme-Linked Immunosorbent Assay (ELISA) Quantitative Assay of Immunoglobulin G. *Immunochemistry* **1971**, *8*, 871−874.

(4) Nilsson, B. Enzyme-Linked Immunosorbent Assays. *Curr. Opin. Immunol.* **1989**, *2*, 898−904.
(5) Zhang, Y.; Guo, Y.; Xianyu, Y.; Chen, W.; Zhao, Y.; Jiang, X. Nanomaterials for Ultra-sensitive Protein Detection. *Adv. Mater.* **2013**, *25*, 3802−3819.
(6) Gopinath, S. C. B.; Tang, T.-H.; Citartan, M.; Chen, Y.; Lakshmipriya, T. Current Aspects in Immunosensors. *Biosens. Bioelectron.* **2014**, *57*, 292−302.
(7) Gao, L.; Zhuang, J.; Nie, L.; Zhang, J.; Zhang, Y.; Gu, N.; Wang, T.; Feng, J.; Yang, D.; Perrett, S.; Yan, X. Intrinsic Peroxidase-like Activity of Ferromagnetic Nanoparticles. *Nat. Nanotechnol.* **2007**, *2*, 577−583.
(8) Chen, W.; Chen, J.; Liu, A.-L.; Wang, L.-M.; Li, G.-W.; Lin, X.-H. Peroxidase-like Activity of Cupric Oxide Nanoparticle. *Chem. Catal. Chem.* **2011**, *3*, 1151−1154.
(9) Asati, A.; Santra, S.; Kaittanis, C.; Nath, S.; Perez, J. M. Oxidase-like Activity of Polymer-Coated Cerium Oxide Nanoparticles. *Angew. Chem., Int. Ed.* **2009**, *48*, 2308−2312.
(10) Song, Y.; Qu, K.; Zhao, C.; Ren, J.; Qu, X. Graphene Oxide: Intrinsic Peroxidase Catalytic Activity and Its Application to Glucose Detection. *Adv. Mater.* **2010**, *22*, 2206−2210.
(11) He, W.; Wu, X.; Liu, J.; Hu, X.; Zhang, K.; Hou, S.; Zhou, W.; Xie, S. Design of AgM Bimetallic Alloy Nanostructures (M = Au, Pd, Pt) with Tunable Morphology and Peroxidase-like Activity. *Chem. Mater.* **2010**, *22*, 2988−2994.
(12) He, W.; Liu, Y.; Yuan, J.; Yin, J.-J.; Wu, X.; Hu, X.; Zhang, K.; Liu, J.; Chen, C.; Ji, Y.; Guo, Y. Au@Pt Nanostructures as Oxidase and Peroxidase Mimetics for use in Immunoassays. *Biomaterials* **2011**, *32*, 1139−1147.
(13) Lien, C.-W.; Huang, C.-C.; Chang, H.-T. Peroxidase-Mimic Bismuth-Gold Nanoparticles for Determining the Activity of Thrombin and Drug Screening. *Chem. Commun.* **2012**, *48*, 7952−7954.
(14) A sphere of 30 nm Fe_3O_4 was crystallographycally drawn and the number of Fe^{2+}/Fe^{3+} atoms were estimated to be ∼25000.
(15) Popescu, D.-L.; Chanda, A.; Stadler, M.; de Oliveira, F. T.; Ryabov, A. D.; Münck, E.; Bominaar, E. L.; Collins, T. J. High-Valent First-Row Transition-Metal Complexes of Tetraamido (4N) and Diamidodialkoxido or Diamidophenolato (2N/2O) Ligands: Synthesis, Structure, and Magnetochemistry. *Coord. Chem. Rev.* **2008**, *252*, 2050−2071.
(16) Ghosh, A.; Mitchell, D. A.; Chanda, A.; Ryabov, A. D.; Popescu, D. L.; Upham, E. C.; Collins, G. J.; Collins, T. J. Catalase−Peroxidase Activity of Iron(III)−TAML Activators of Hydrogen Peroxide. *J. Am. Chem. Soc.* **2008**, *130*, 15116−15126.
(17) Ellis, W. C.; Tran, C. T.; Denardo, M. A.; Fischer, A.; Ryabov, A. D.; Collins, T. J. Design of More Powerful Iron-TAML Peroxidase Enzyme Mimics. *J. Am. Chem. Soc.* **2009**, *131*, 18052−18053.
(18) Collins, T. J.; Gordon-Wylie, S. W. Long-Lived Homogenous Oxidation Catalysts. US Patent No. US5,847,120, December 8th, 1998.
(19) Panda, C.; Ghosh, M.; Panda, T.; Banerjee, R.; Sen Gupta, S. Fe(III) Complex of Biuret-Amide Based Macrocyclic Ligand as Peroxidase Enzyme Mimic. *Chem. Commun.* **2011**, *47*, 8016−8018.
(20) Ghosh, M.; Singh, K. K.; Panda, C.; Weitz, A.; Hendrich, M. P.; Collins, T. J.; Dhar, B. B.; Sen Gupta, S. Formation of a Room Temperature Stable FeV(O) Complex: Reactivity Toward Unactivated C−H Bonds. *J. Am. Chem. Soc.* **2014**, *136*, 9524−9527.
(21) (a) Malvi, B.; Panda, C.; Dhar, B. B.; Gupta, S. S. One Pot Glucose Detection by [FeIII(biuret-amide)] Immobilized on Mesoporous Silica Nanoparticles: An Efficient HRP Mimic. *Chem. Commun.* **2012**, *48*, 5289−5291. (b) Huh, S.; Wiench, J. W.; Yoo, J. C.; Pruski, M.; Lin, V.S-Y. Organic Functionalisation and Morphology Control of Mesoporous Silicas via a Co-Condensation Synthesis Method. *Chem. Mater.* **2003**, *15*, 4247−4256.
(22) Panda, C.; Dhar, B. B.; Malvi, B.; Bhattacharjee, Y.; Gupta, S. S. Catalytic Signal Amplification using [FeIII(biuret-amide)]-Mesoporous Silica Nanoparticles: Visual Cyanide Detection. *Chem. Commun.* **2013**, *49*, 2216−2218.
(23) Schlossbauer, A.; Schaffert, D.; Kecht, J.; Wagner, E.; Bein, T. Click Chemistry for High-Density Biofunctionalization of Mesoporous Silica. *J. Am. Chem. Soc.* **2008**, *130*, 12558−12559.
(24) Nakazawa, J.; Stack, T. D. P. Controlled Loadings in a Mesoporous Material: Click-on Silica. *J. Am. Chem. Soc.* **2008**, *130*, 14360−14361.
(25) Josephy, P. D.; Eling, T.; Mason, R. P. The Horseradish Peroxidase-Catalyzed Oxidation of 3,5,3′,5′-tetramethylbenzidine. Free Radical and Charge-Transfer Complex Intermediates. *J. Biol. Chem.* **1982**, *257*, 3669−75.
(26) Ellis, W. C.; Tran, C. T.; Roy, R.; Rusten, M.; Fischer, A.; Ryabov, A. D.; Blumberg, B.; Collins, T. J. Designing Green Oxidation Catalysts for Purifying Environmental Waters. *J. Am. Chem. Soc.* **2010**, *132*, 9774−9781.
(27) Chanda, A.; Shan, X.; Chakrabarti, M.; Ellis, W. C.; Popescu, D. L.; Tiago de Oliveira, F.; Wang, D.; Que, L.; Collins, T. J.; Münck, E.; Bominaar, E. L. (TAML)Fe^{IV}=O Complex in Aqueous Solution: Synthesis and Spectroscopic and Computational Characterization. *Inorg. Chem.* **2008**, *47*, 3669−3678.
(28) Gupta, S. S.; Stadler, M.; Noser, C. A.; Ghosh, A.; Steinhoff, B.; Lenoir, D.; Horwitz, C. P.; Schramm, K.-W.; Collins, T. J. Rapid Total Destruction of Chlorophenols by Activated Hydrogen Peroxide. *Science* **2002**, *296*, 326−328.
(29) Green, N. M. Avidin and Streptavidin. In *Methods in Enzymology*; Meir, W., Edward, A. B., Eds.; Academic Press: New York, 1990; Vol. *184*, pp51−67.
(30) Pradhan, K.; Gadgil, M. Effect of Addition of 'Carrier' DNA During Transient Protein Expression in Suspension CHO Culture. *Cytotechnology* **2012**, *64*, 613−622.
(31) Eum, J. Y.; Hwang, S. Y.; Ju, Y.; Shim, J. M.; Piao, Y.; Lee, J.; Kim, H.-S.; Kim, J. A Highly Sensitive Immunoassay Using Antibody-Conjugated Spherical Mesoporous Silica with Immobilized Enzymes. *Chem. Commun.* **2014**, *50*, 3546−3548.